

# Zircon U-Pb dating on the Mesozoic volcanic suite from the Qingshan Group stratotype section in eastern Shandong Province and its tectonic significance

LING WenLi<sup>1,2†</sup>, XIE XianJun<sup>1,2</sup>, LIU XiaoMing<sup>1,3</sup> & CHENG JianPing<sup>1</sup>

<sup>1</sup> Faculty of Earth Sciences, China University of Geosciences, Wuhan 430074, China;

<sup>2</sup> State Key Laboratory of Geological Processes and Mineral Resources, China University of Geosciences, Wuhan 430074, China;

<sup>3</sup> Key Laboratory of Continental Dynamics, Northwest University, Xi'an 710069, China

**A geochronological study of zircon U-Pb on the volcanic rocks from the stratotype section of the Qingshan Group within the Jiaozhou Basin, eastern Shandong Province, is presented. The zircons were analyzed using the method of *in situ* ablation of a 193 nm excimer laser system coupled with an up to date ICP-MS system. Among the three formations of the Qingshan Group, zircons recovered from the lowest part of the Houkuang Fm. were dated at  $106\pm 2$  Ma (95% confidence, the same below), whereas those from the lower and upper parts of the Shiqianzhuang Fm. were given ages of  $105\pm 4$  Ma and  $98\pm 1$  Ma, respectively. A spatially decreasing trend for the Mesozoic magmatic timing from west to east in the province is observed through comparing the data of this study with those by previous works on the Qingshan volcanic lavas occurring at western Shandong and within the Yishu fault zone. The Qingshan volcanic rocks are constituent of the 'Shoshonite Province' in East China. Exposed at most provinces of central East China along the Tan-Lu fault and the Yangtze fault zones, these volcanic suites are characterized by shoshonite and high-K calcalkalic rocks in lithology and thought to be correlated with the partial melting of continental mantle in genesis. It is also shown that the Qingshan potassic volcanic suite from eastern Shandong basins is distinctly younger than those from other areas of the shoshonite province. By contrary, ages of the Mesozoic to Cenozoic alkaline basalts, sourced by asthenospheric mantle, from both northern Huaiyan basin and northern Dabie belt along the Tan-Lu fault zone and from the Ningwu, Lishui and Luzong basins along the Yangtze fault zone are observably older than those occurring within eastern Shandong. The revealed temporal and spatial patterns in magmatism for the two types of volcanic suites make an important geochronological constraint on the Mesozoic to Cenozoic dynamic evolution model of the subcontinental lithosphere in East China.**

Mesozoic volcanic suite, Qingshan Group, stratotype section, zircon U-Pb, tectonic significance

Lower continental crust and/or subcontinental lithospheric mantle delamination along with flux ascending erosion of asthenosphere to lithosphere are thought as one of the most important mechanisms for crust-mantle interaction, exchange and recycling. The processes are suggested playing a role in the continental crust growth and evolution as significant as those by plate converging subduction along oceanic boundary (referring to a re-

view by ref. [1]). However, our understanding on the subcontinental lithospheric delamination and underplating erosion is relatively limited compared with those described in the plate tectonic theory. Wherefore, learn-

Received May 20, 2005; accepted July 28, 2005

doi: 10.1007/s11430-007-2065-6

<sup>†</sup>Corresponding author (email: wlling@cug.edu.cn)

Supported by the National Natural Science Foundation of China (Grant No. 40133020) and Innovation Term Grant of Ministry of Education of China

ing about subcontinental delamination and underplating is the key to understanding Earth's composition, evolution and their crust-mantle systems as well as to setting up Earth's dynamic evolutionary model<sup>[2-4]</sup>.

Collisions between the North China craton and its adjacent continental blocks during the late Paleozoic to early Mesozoic led to the unification of eastern Asian, where East China is enclosed. A series of geological events during a period of the Jurassic to Cretaceous indicated by lithospheric thinning and regional tectonic transition feature the newly formed East China, which is coupled with blustering igneous activities ranging from Mesozoic to Cenozoic. The Mesozoic-Cenozoic abrupt transform in subcontinental lithosphere thickness, regional tectonic alignment and magmatic activity in East China has been interpreted as an expression of the subcontinental lithospheric delamination and ascending erosion by asthenospheric flux<sup>[5,6]</sup>. To learn the processes that occurred deeply within the subcontinental lithosphere, the most direct evidence comes from xenoliths originated from the lower part of the lithosphere, i.e. constituent rocks of lower crust and lithospheric mantle, representative of their chemical compositions. However, due to the factors such as limited spatiotemporal distribution, small size as well as heterogeneity in lower crust and subcontinental lithospheric mantle (SCLM), the xenolith application is restricted. Igneous rocks originated from lower crust and SCLM with their relatively wide occurrence, therefore, are especially valuable in investigation of regional lithospheric evolution<sup>[7]</sup>.

Since the argument in the early 1990s that ~120 km root part of the lithosphere beneath the North China craton had been lost during the Mesozoic<sup>[8-10]</sup>, prominent research progress on the lithospheric evolution in East China has been achieved. A general evolution model on lithospheric thickness of the North China craton was proposed suggesting a transition from ~200 km in the Paleozoic, decreasing to ~60 km in the Mesozoic, and re-accreted up to ~60 km coupled with a SCLM replacement or transform<sup>[8-11]</sup>. Gao et al.<sup>[12]</sup> displayed plausible geochemical evidence revealing that Jurassic lavas occurring at the northern North China craton originated from partial melting of eclogitic rocks, followed by a delamination of the lower crust foundering into the upper mantle beneath the North China craton. Various workers argued that source rocks parental to the Cenozoic alkaline basalts in South China are distinct

from their counterpart in North China, i.e. the basalts in South China were sourced by melt mixtures originated from depleted asthenospheric mantle, DM and a EM II component of enriched SCLM character, but those in North China by mixtures of DM and EM I of SCLM character<sup>[8,13-15]</sup>. However, detailed understandings are still deficient in regard to the Mesozoic to Cenozoic lithospheric evolution in East China, e.g. if the mafic lower crust and the SCLM broke off contemporarily during the lithospheric delamination. What is the inducing factor or event causing the delamination? How large the size was for the lower part delamination of the lithosphere beneath northern East China and whether there is an asynchrony when diverse delaminated sections foundering into the upper mantle? It is evident that the answers to these questions are the key to understanding the processes of crust-mantle interactions, recycling and crustal growth as well as to particularly constructing the Mesozoic-Cenozoic lithospheric dynamic evolution model in East China. To have plausible answers to these questions, detailed investigations on the timing, spatial distribution and petrogenesis of diverse igneous suites from their major outcrops in East China are essential.

This study represents a geochronological research using the zircon U-Pb method on the volcanic suite of the Cretaceous Qingshan Group from the Jiaozhou basin, eastern Shandong Province. Through comparing the data by this study with those of the Qingshan volcanic suites from the western Shandong and Yishu fault zone by previous workers, a spatiotemporal trend for the Qingshan volcanic rocks in Shandong Province is discussed. Coupled with a summary on temporal variation of the 'Shoshonite Province' in East China, a geochronological constraint on the source magma change and regional tectonic alignment shift during the period of Mesozoic to Cenozoic in East China, especially in the North China craton is given.

## 1 Geological setting

In East China, Shandong Province is one of the major regions where Mesozoic-Cenozoic volcanic suites are well developed. The province is separated into two parts geologically, the eastern and western units by the Tan-Lu fault zone, locally called the Yishu zone, with a NNE trending and extending into the sea at its northernmost end (Figure 1(a)). In the western unit, relatively com-

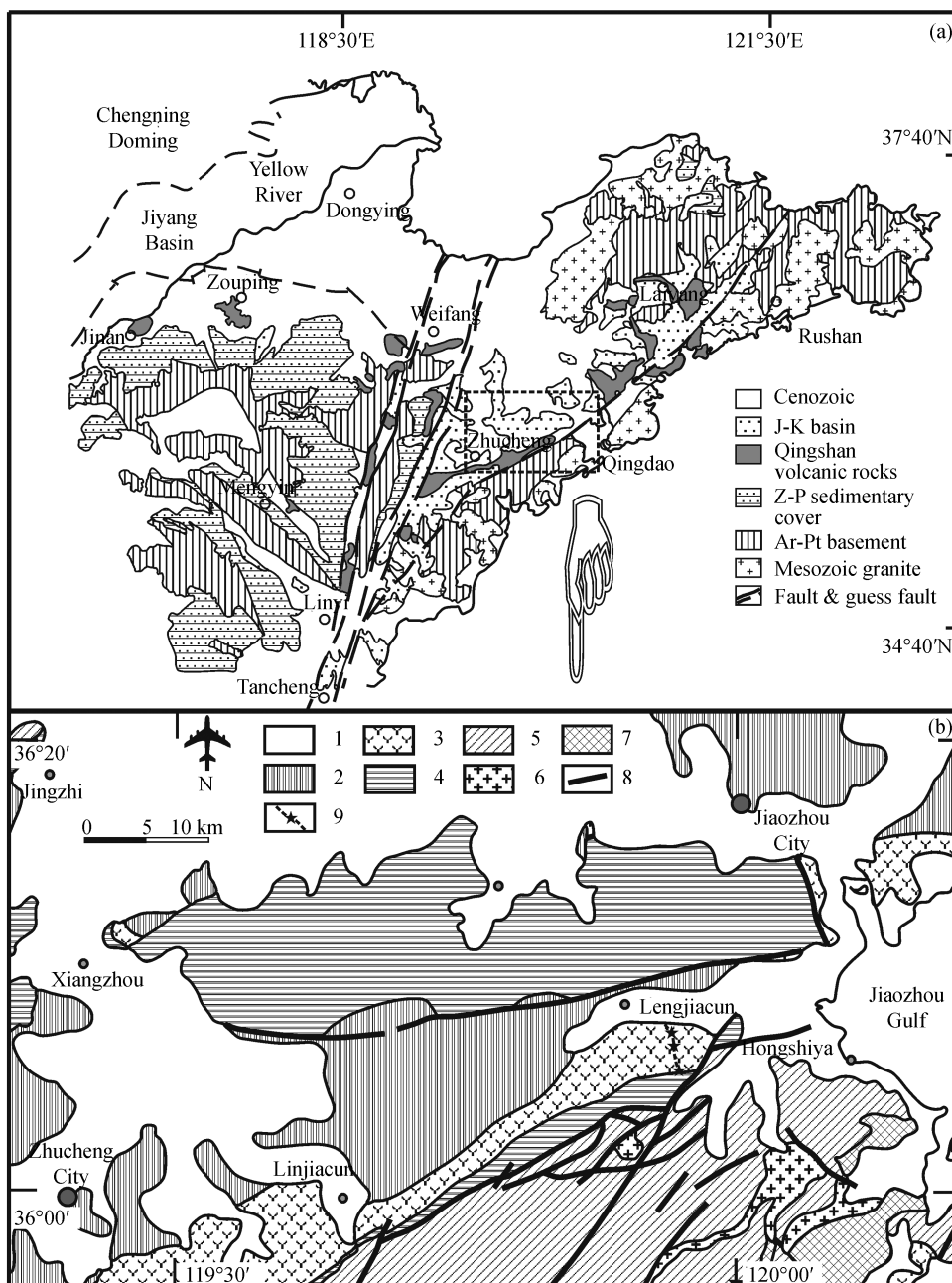


**Figure 1** Schematic geological maps of Shandong Province (a) and the Jiaozhou basin (b) (modified after ref. [16]). 1, Quaternary System; 2, Mesozoic Wangsi Group; 3, Mesozoic Qingshan Group; 4, Mesozoic Laiyang Group; 5, Precambrian basement; 6, Yanshanian granite; 7, Yanshanian syenite-monzonite; 8, fault; 9, field trip section and sampling location.

plete strata from the Archean-Proterozoic basement, Paleozoic marine facies strata and Mesozoic-Cenozoic sedimentary-volcanic rocks are developed, typical of the North China stratigraphy; whereas in the eastern unit, it is characterized by a binary-structure of strata, i.e. the Archean-Proterozoic basement is directly covered by Mesozoic-Cenozoic volcanic-sedimentary rocks of terrestrial facies, missing Paleozoic stratum<sup>[16]</sup>. Despite a

dissimilarity in Precambrian-Paleozoic strata, the distributions of the Mesozoic-Cenozoic volcanic-sedimentary strata both in the eastern and western units are strictly controlled by regional fault belts, coupled with a trend shifting of the sedimentary basins from EW to NNE coinciding with a transform of regional tectonic alignment from a north-south compressing to a northwest-southeast extending. This coherence between the basin extending

and the regional tectonic alignment is common in East China<sup>[11,17–19]</sup>.

After the suturing between the North China and Yangtze cratons, the Mesozoic-Cenozoic volcanic-sedimentary strata in Shandong Province were developed along the regional fault belts and their adjacent areas, which are separated into three stratigraphic subregions, i.e. the eastern and western subregions, east and west of the Yishu fault zone, respectively, and the Yishu Fault subregion boarded by the Tangwu-Gegou and Changyi-Dadian faults<sup>[16]</sup>. The Mesozoic volcanic lavas mainly occur within the Qingshan Group, which is underlain and overlain by the terrestrial facies strata of Wangshi and Laiyang Groups, respectively. Based on the field geological survey of more than one decade documenting, Zhang and Liu<sup>[20]</sup> and Liu et al.<sup>[21]</sup> suggested that the stratum of the Qingshan Group exposed in the three subregions equivalent or comparable, and is subdivided into four formations, i.e. Houkuang, Bamudi, Shiqianzhuang and Fanggezhuang Formations, from the lower stratum upward. However, the development of the stratum is variable among these subregions: all four formations are well exposed in the eastern subregion (e.g. Jiaolai basin), whereas in the western subregion, only the Bamudi and Fanggezhuang Formations are observed (e.g. Mengyin basin). The Qingshan stratum within the Yishu fault zone shows a transition between the eastern and western subregions (e.g. Qibaoshan and Fenlingshan areas in Wulian County).

## 2 Samples and analysis method

Zircon-host rocks for the U-Pb dating were selected from a sampling set from a ~10 km stratigraphic section northward from Hexiguo to Yanghezhen in the Jiaozhou basin, one of the Qingshan Group stratotype sections in the eastern subregion, ~23 km southwest of Jiaozhou City (Figure 1(b)). Due to a relatively completed occurrence in stratigraphy, 30 whole rock volcanic samples were collected along the trip section. Among them, three samples were selected for zircon mineral separation, i.e. a mauve rhyolite sample MJZ-ZC-01 (locus GPS reading 119°54.869'E, 36°04.755'N) from the base part of the Houkuang Fm., a maroon rhyolite sample MJZ-ZC-02 (119°54.511'E, 36°05.602'N) and a dust-colour dacite sample MJZ-ZC-03 (119°54.476'E, 36°06.471'N) from the lower and upper parts of the Shiqianzhuang Fm., respectively. Heavy minerals were concentrated using

concentrating table from medium-granular size grains broken from ~20 kg whole rock samples. Zircon separates were hand-picked under a microscope from refined grains using wet elutriation by handwork. To prevent potential sample-cross contamination, fully cleaning to the shaking table and elutriation pans was carried out before each process to start zircon selection.

Most zircon grains are relatively uniform in shape of small short prismatic crystals with 50–100 μm×100–250 μm, mostly euhedral with minor anhedral. Under the cathodoluminescence (CL) examination, zircons show well-developed oscillatory compositional zoning typically found in zircons crystallised from magmatic melts (Figure 2(a)–(d)). It is notable that some zircon crystals of MJZ-ZC-03 dacite from the Upper Shiqianzhuang Fm. display secondary accreted rims. However, the smooth and sharpness contacts between the rim and their mantle indicate that the mantle parts of these crystals had not suffered evident re-sorbing (Figure 2(e)–(f)).

To avoid a bias analysis, zircons with various size and length/width ratio were selected for U-Pb dating. The minerals were stuck linearly on the double-face adhesive tape by tweezers under a binocular and put into a circular plastic mould, where epoxy resin was poured in. After solidification of the epoxy resin, the surface contacting the adhesive tape was polished to smoothly expose crystal interiors of the zircons. CL image photos of the polished zircons were taken for analysis point selection during the U-Pb *in situ* measurement. CL photos were finished at Beijing Institute of Geology and Geophysics, Chinese Academy of Sciences.

U-Pb isotopic analysis was completed at the Continental Dynamics Laboratory, Geological Department of Northwest University in Xi'an using the technique of laser ablation-ICPMS (LA-ICPMS). The laser ablation system was made by German MicroLas Company, GeoLas 200M, in which a laser generator, ComPex102, from Lambda Physik Company with a 193 nm ArF excimer optical maser was equipped. Zircon microparticles created by laser ablation were carried into an ICPMS system, 7500a by the Agilent. Due to adopting a new technique of Shield Touch, the ICPMS system used in this study shows some ten times higher sensitivity than other average systems. The higher sensitivity of the system improved the data quality, which is adequately manifested in Table 1.

During the U-Pb analysis, the size of laser spot is set



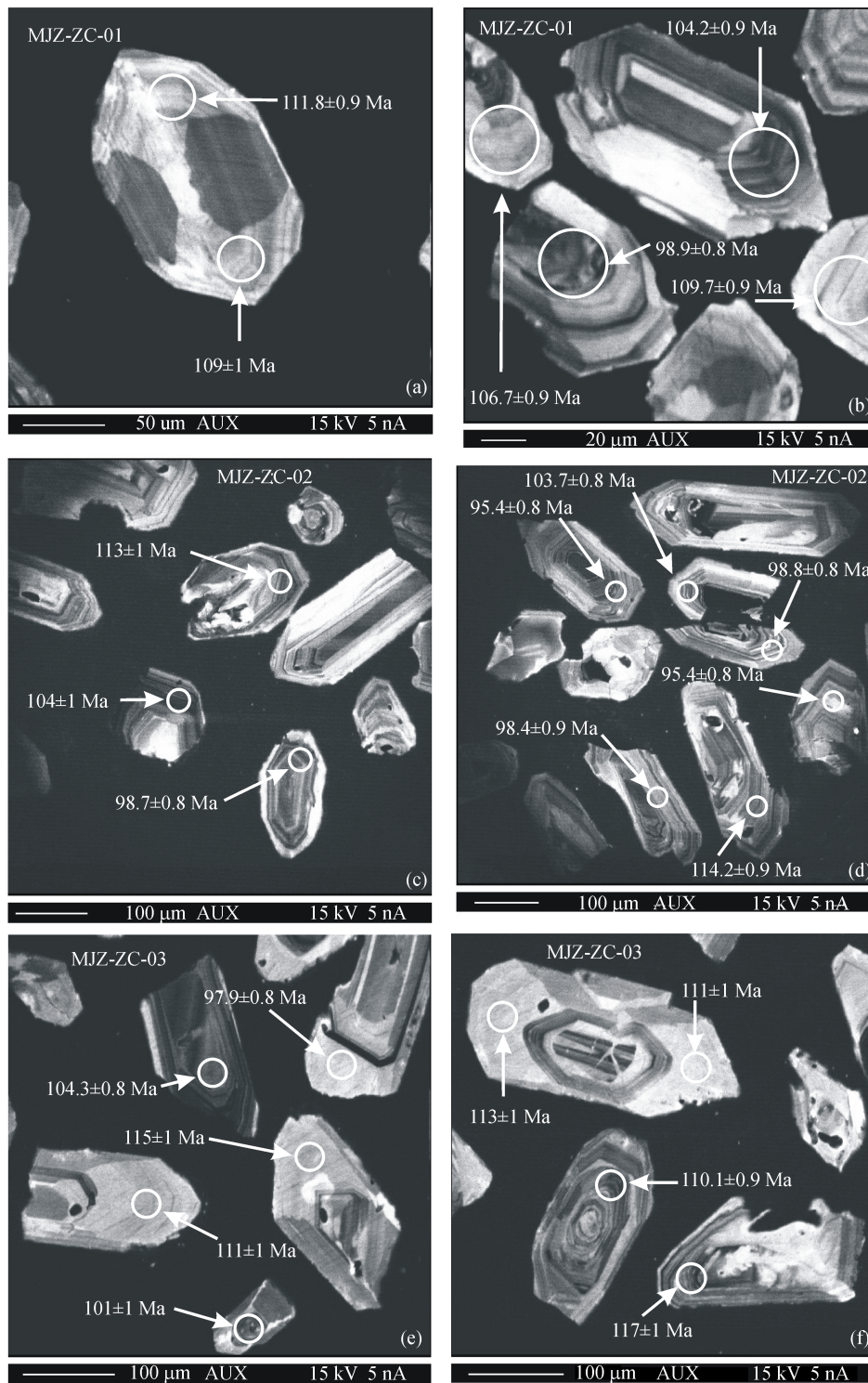


**Figure 2** Cathodoluminescence images, analyzed spots and their  $^{206}\text{Pb}/^{238}\text{U}$  ages of Qingshan zircons from the Jiaozhou basin by LA-ICPMS. (a), (b) MJZ-ZC-01; (c), (d) MJZ-ZC-02; (e), (f) MJZ-ZC-3.

to 30  $\mu\text{m}$ , following a sequence of 30–50 seconds for blank, 60 seconds of laser ablation and data collection. Zircon standard of 91500, used for correction of mass discrimination, was analyzed at intervals of 5–7 sample

zircon analyses. The raw data of the isotopic composition were treated using the software of Glitter (Rev. 4.0), whereas a common Pb correction was made following the method described by Andersen<sup>[22]</sup> using a template

**Table 1** U-Pb composition and apparent age of Qingshan Group zircons in Jiaozhou basin

Analysis number	Isotopic ratio <sup>a)</sup>								Apparent age (Ma) <sup>b)</sup>		Concordance <sup>c)</sup>
	<sup>207</sup> Pb/ <sup>206</sup> Pb±1σ		<sup>207</sup> Pb/ <sup>235</sup> U±1σ		<sup>206</sup> Pb/ <sup>238</sup> U±1σ		<sup>208</sup> Pb/ <sup>232</sup> Th±1σ		<sup>206</sup> Pb/ <sup>238</sup> U±1σ		
MJZ-ZC-01											
ZC-01.1	0.04783	0.00107	0.11123	0.00234	0.01687	0.00013	0.00607	0.00007	107.8	0.8	1.00
ZC-01.2	0.04782	0.00348	0.11107	0.00802	0.01684	0.00016	0.00557	0.00015	107.7	1	1.00
ZC-01.3	0.05002	0.00290	0.10966	0.00626	0.01590	0.00017	0.00502	0.00003	102.0	1	0.98
ZC-01.4	0.04786	0.00234	0.11715	0.00564	0.01775	0.00015	0.00682	0.00012	113.4	1	1.01
ZC-01.6	0.04780	0.00059	0.10756	0.00099	0.01632	0.00013	0.00565	0.00003	104.4	0.8	1.00
ZC-01.7	0.04780	0.00106	0.10734	0.00220	0.01629	0.00013	0.00563	0.00005	104.2	0.9	1.00
ZC-01.8	0.04784	0.00158	0.11318	0.00360	0.01716	0.00015	0.006937	0.00035	109.7	0.9	1.00
ZC-01.9	0.04778	0.00067	0.10548	0.00119	0.01601	0.00013	0.00538	0.00003	102.4	0.8	1.00
ZC-01.10	0.04782	0.00233	0.11002	0.00529	0.01669	0.00014	0.00645	0.0001	106.7	0.9	1.00
ZC-01.11	0.04776	0.00224	0.10184	0.00470	0.01547	0.00013	0.00553	0.00011	98.9	0.8	1.00
ZC-01.12	0.04780	0.00099	0.10825	0.00206	0.01642	0.00014	0.00545	0.00004	105.0	0.9	1.00
ZC-01.13	0.04783	0.00237	0.11162	0.00545	0.01693	0.00014	0.00685	0.00011	108.2	0.9	1.01
ZC-01.15	0.04782	0.00114	0.11093	0.00247	0.01682	0.00014	0.00608	0.00006	107.5	0.9	1.00
ZC-01.16	0.04781	0.00085	0.10845	0.00169	0.01645	0.00014	0.00567	0.00004	105.2	0.9	1.00
ZC-01.17	0.04785	0.00131	0.11513	0.00299	0.01745	0.00015	0.00563	0.00005	111.5	0.9	1.00
ZC-01.21	0.04775	0.00226	0.10109	0.00471	0.01535	0.00013	0.00522	0.00009	98.2	0.8	1.00
ZC-01.23	0.04782	0.00058	0.10992	0.00100	0.01667	0.00013	0.00552	0.00003	106.6	0.8	1.00
ZC-01.24	0.04779	0.00142	0.10652	0.00305	0.01617	0.00013	0.00565	0.00005	103.4	0.8	1.00
ZC-01.25	0.04785	0.00180	0.11491	0.00423	0.01742	0.00014	0.00584	0.00009	111.3	0.9	1.01
ZC-01.26	0.04912	0.00204	0.11519	0.00465	0.01701	0.00017	0.00538	0.00003	109.0	1	0.99
ZC-01.28	0.05025	0.00265	0.11895	0.00616	0.01717	0.00017	0.00542	0.00003	110.0	1	0.98
ZC-01.29	0.04786	0.00159	0.11666	0.00374	0.01768	0.00015	0.00575	0.00007	113.0	1	1.00
MJZ-ZC-02											
ZC-02.3	0.04889	0.00051	0.11667	0.00103	0.01732	0.00014	0.00628	0.00003	110.7	0.9	0.99
ZC-02.7	0.04923	0.00050	0.09770	0.00082	0.01440	0.00012	0.00567	0.00003	92.2	0.8	0.99
ZC-02.8	0.04915	0.00051	0.12430	0.00108	0.01835	0.00015	0.00617	0.00003	117.2	0.9	0.99
ZC-02.9	0.04782	0.00099	0.10965	0.00207	0.01663	0.00014	0.00533	0.00003	106.3	0.9	1.00
ZC-02.10	0.04928	0.00050	0.11052	0.00093	0.01627	0.00014	0.00626	0.00003	104.0	0.9	0.99
ZC-02.11	0.04775	0.00075	0.10157	0.00135	0.01543	0.00013	0.00510	0.00004	98.7	0.8	1.00
ZC-02.13	0.04786	0.00066	0.11671	0.00131	0.01769	0.00014	0.00678	0.00004	113.0	0.9	1.00
ZC-02.16	0.04830	0.00159	0.11256	0.00356	0.01690	0.00015	0.00536	0.00003	108.0	1	1.00
ZC-02.18	0.04899	0.00052	0.12574	0.00112	0.01862	0.00016	0.00587	0.00003	119.0	1	1.00
ZC-02.20	0.04777	0.00087	0.10312	0.00168	0.01566	0.00013	0.00557	0.00006	100.2	0.8	1.00
ZC-02.21	0.04783	0.00080	0.11168	0.00162	0.01694	0.00014	0.00606	0.00004	108.3	0.9	1.00
ZC-02.22	0.04775	0.00201	0.10123	0.00416	0.01537	0.00014	0.00489	0.00003	98.4	0.9	1.00
ZC-02.23	0.04910	0.00051	0.12093	0.00106	0.01787	0.00015	0.00602	0.00003	114.2	0.9	0.99
ZC-02.24	0.04809	0.00050	0.10232	0.00089	0.01544	0.00013	0.00474	0.00002	98.8	0.8	1.00
ZC-02.26	0.04779	0.00062	0.10692	0.00106	0.01622	0.00013	0.00575	0.00003	103.7	0.8	1.00
ZC-02.27	0.04772	0.00062	0.09810	0.00097	0.01491	0.00013	0.00481	0.00003	95.4	0.8	1.00
ZC-02.30	0.04899	0.00051	0.12537	0.00112	0.01856	0.00016	0.00559	0.00003	119.0	1	1.00
MJZ-ZC-03											
ZC-03.2	0.04775	0.00496	0.10077	0.01042	0.01531	0.00014	0.00565	0.00017	97.9	0.9	1.00
ZC-03.14	0.06415	0.00071	0.14746	0.00137	0.01667	0.00014	0.00454	0.00002	106.6	0.9	0.87
ZC-03.15	0.07066	0.00071	0.16785	0.00138	0.01723	0.00014	0.00480	0.00002	110.1	0.9	0.83
ZC-03.17	0.08605	0.00111	0.20907	0.00239	0.01762	0.00015	0.00516	0.00003	112.6	1	0.76
ZC-03.18	0.08033	0.00261	0.19151	0.00594	0.01729	0.00017	0.00526	0.00004	111.0	1	0.79
ZC-03.19	0.07797	0.00326	0.18950	0.00766	0.01763	0.00019	0.00537	0.00005	113.0	1	0.80
ZC-03.20	0.08182	0.00441	0.19619	0.01033	0.01739	0.00020	0.00528	0.00005	111.0	1	0.78
ZC-03.21	0.08846	0.00579	0.22136	0.01421	0.01815	0.00023	0.00548	0.00007	116.0	1	0.76
ZC-03.22	0.09036	0.00309	0.21887	0.00713	0.01757	0.00018	0.00530	0.00005	112.0	1	0.75
ZC-03.23	0.07152	0.00930	0.16405	0.02119	0.01663	0.00025	0.00510	0.00009	106.0	2	0.83
ZC-03.24	0.08927	0.00598	0.22717	0.01489	0.01846	0.00025	0.00557	0.00006	118.0	2	0.75

a) Common Pb corrected using the method by Andersen<sup>[22]</sup>; b) apparent ages were calculated using Isoplot/Ex (rev. 2.49) by Ludwig<sup>[23]</sup>; c) concordance is defined as the square root of age ratio <sup>206</sup>Pb/<sup>238</sup>U to <sup>207</sup>Pb/<sup>206</sup>Pb.

running in MS Excel provided by the author. U-Pb geochronological calculation used Isoplot/Ex (rev. 2.49) by Ludwig<sup>[23]</sup>. During this analysis session, the 91500 zircon standard gives concordant U-Pb isotopic compositions with an average  $^{206}\text{Pb}/^{238}\text{U}$  apparent age of  $1062.6\pm 3.3\text{Ma}$  (95% confidence,  $n=23$ , MSWD=0.034), while the average  $^{206}\text{Pb}/^{238}\text{U}$  apparent age for TEM zircon standard is  $417\pm 12\text{Ma}$  (95% confidence,  $n=4$ , MSWD=5.4).

### 3 Zircon U-Pb geochronology

The zircon U-Pb composition,  $^{206}\text{Pb}/^{238}\text{U}$  apparent age and their concordant feature of the three Qingshan volcanic rocks are listed in Table 1. In the table, the concordance is defined as square root of apparent age ratio of  $^{206}\text{Pb}/^{238}\text{U}$  to  $^{207}\text{Pb}/^{206}\text{Pb}$ <sup>1)</sup>. Concordia diagrams for these samples are shown in Figure 3. Due to the growth of  $^{207}\text{Pb}/^{235}\text{U}$  resulting from the radioactive decay since the  $\sim 0.8$  Ga is relatively minimal, it is difficult for young zircons to discriminate the concordant ages from ages representative of variable Pb losing in a normal concordia plot of  $^{206}\text{Pb}/^{238}\text{U}$  vs.  $^{207}\text{Pb}/^{235}\text{U}$ . Alternatively, the Tera-Wasserburg concordia diagram, i.e.  $^{238}\text{U}/^{206}\text{Pb}$  vs.  $^{207}\text{Pb}/^{206}\text{Pb}$  plot, is adopted to illustrate the U-Pb concordant characters of the young zircons.

Zircons from the MJZ-ZC-01 show a concordant U-Pb isotopic composition with a concordance range of 0.98–1.01 (Figure 3(a)). The whole data of  $^{206}\text{Pb}/^{238}\text{U}$  ratio yield a weighted average apparent age of  $106\pm 2$  Ma (95% confidence, the same below). It is notable that the MSWD for the average  $^{206}\text{Pb}/^{238}\text{U}$  age is as high as 22, which is interpreted as resulting from the higher sensitivity of 7500a ICPMS relative to other average systems. When the analysis error is to be enlarged 2–3 times, which is still evidently better than those by typical ICPMS systems, the recalculated MSWD decreased dramatically to 5.5–2.5. Therefore, the reason for the elevated MSWD value is suggested coming from the improved analysis precision by the new ICPMS system, which also causes a decreasing in overlap, even separating between the analysis error ellipses in the concordia diagrams.

Sample MJZ-ZC-02 also shows a concordant U-Pb composition for its zircons with a concordance ranging

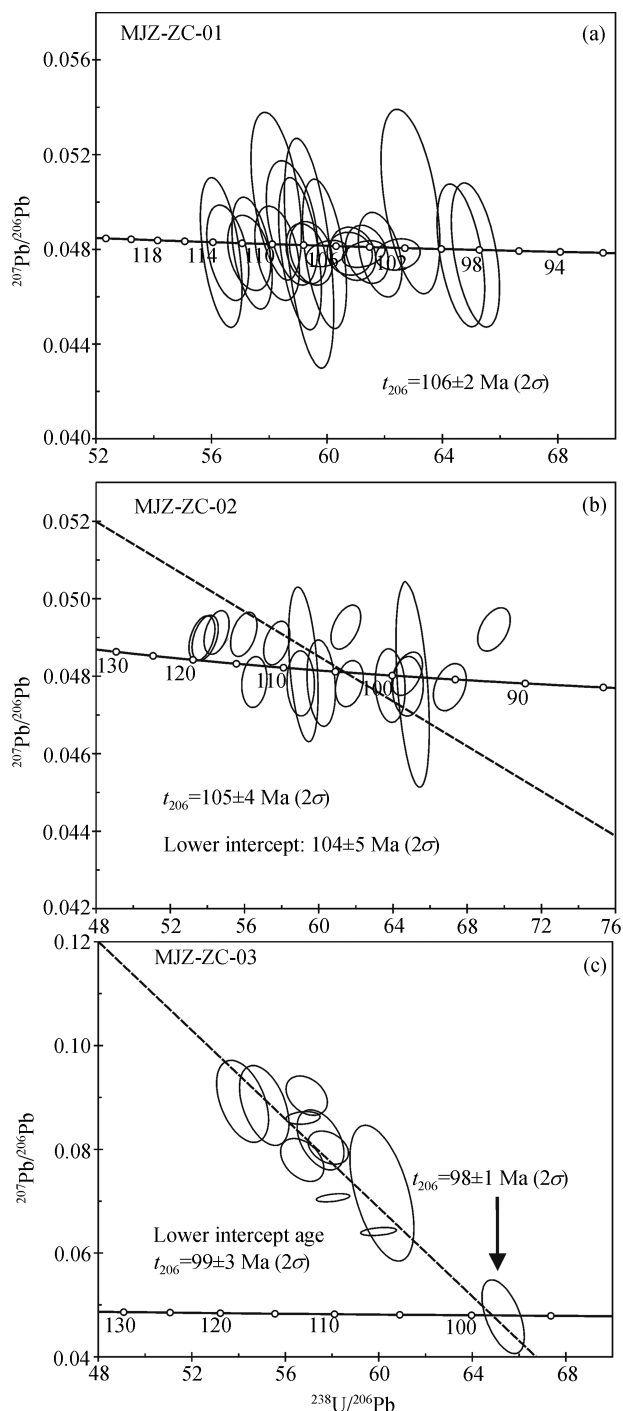


**Figure 3**  $^{238}\text{U}/^{206}\text{Pb}$ - $^{207}\text{Pb}/^{206}\text{Pb}$  concordia diagrams of Qingshan zircons from the Jiaozhou basin.

from 0.99 to 1.0 (Figure 3(b)). The zircons give an average  $^{206}\text{Pb}/^{238}\text{U}$  age of  $105\pm 4$  Ma, a slightly bigger error in age than that of the MJZ-ZC-01. A lower intercept age of  $104\pm 5$  Ma (95% confidence, the same below) is also obtained, showing a good agreement with the  $^{206}\text{Pb}/^{238}\text{U}$

1) Yuan H L. Liquid-sampling and laser ablation ICP-MS and its applications in geochemistry. Ph. D. thesis (in Chinese with English abstract), Wuhan: Graduate School, China Univ Geosci, 2002

age in their analysis error limit.

Sample MJZ-ZC-03 displays a diverse circumstance from the two above samples. Only one zircon grain has concordant U-Pb isotopic composition, while the others exhibit variable degree discordance with a major population ranging from 0.75 to 0.87 in concordance (Figure 3(c)). However, a lower intercept age of  $98 \pm 1$  Ma is obtained, which agrees well with the  $^{206}\text{Pb}/^{238}\text{U}$  age of  $99 \pm 3$  Ma given by the concordant zircon within the limit of their analysis error. Accordingly, the age of  $98 \pm 1$  Ma is regarded as the crystallizing time of the MJZ-ZC-03 dacite rock.

In view of field geology, the decreasing trend in age for the Qingshan volcanic rocks given by the zircon U-Pb dating properly coincides with the constraint of an upward younger evolution from the lower Houkuang Fm. to Shiqianzhuang Fm. of the Qingshan stratigraphy.

## 4 Discussion

Major and trace elemental compositions of the three volcanic samples are listed in Table 2. In a TAS (total alkali vs. silica) diagram (Figure 4(a)), rocks MJZ-ZC-01 and MJZ-ZC-02 fall into the field of rhyolite, but the MJZ-ZC-03 into dacite. Based on the major elemental compositions of the 30 samples along the sampling section (unpublished data by the authors), there are decreasing

and increasing trends in silica and alkali contents, respectively, from the lower part of the Qingshan stratum upward, i.e.  $\text{SiO}_2$  of 70.18–73.97 (% the same below) and  $\text{Na}_2\text{O}+\text{K}_2\text{O}$  of 7.54–9.13 for the Houkuang Fm., 71.34–74.52 and 8.28–9.18 for the lower and middle Shiqianzhuang Fm., 67.58–68.18 and 8.40–9.83 for the upper Shiqianzhuang Fm. On the  $\text{Na}_2\text{O}$  vs.  $\text{K}_2\text{O}$  plot (Figure 4(d)), MJZ-ZC-01 is classed as ultra-potassic rock, while MJZ-ZC-02 and MJZ-ZC-03 as shoshonite. Chondrite normalized<sup>[24]</sup> diagram shows relative enrichment in LREE for all samples and HREE enrichment for the rhyolite from the lower part of the section, along with an increasing in REE content from the rhyolitic to the dacitic (Figure 3(c)). The Jiaozhou volcanic rocks are further characterized by enrichment in LILE (large ion lithophile element) and depletion in HFSE (high field strength element) of Nb, Ta, Ti and P relative to their adjacent elements indicated by a primitive mantle normalization diagram<sup>[24]</sup>, coupled with depleted Sr and enriched K contents (Figure 4(d)).

Potassic volcanic rocks in the Qingshan Group are found in all three subregions of Shandong Province. Moderately comprehensive geochemical studies, including radiometric dating, on the Qingshan volcanic lavas occurring in the Mengyin area of the eastern subregion and the Wulian area in the Yishu fault zone,

**Table 2** Major (%) and trace ( $\mu\text{g/g}$ ) elemental contents of Qingshan volcanic rocks in Jiaozhou basin

Sample	MJZ-ZC-01	MJZ-ZC-02	MJZ-ZC-03	Sample	MJZ-ZC-01	MJZ-ZC-02	MJZ-ZC-03
$\text{SiO}_2$	73.97	73.76	68.18	Zr	264	132	379
$\text{TiO}_2$	0.25	0.22	0.48	Nb	15.8	19.0	26.9
$\text{Al}_2\text{O}_3$	12.97	13.69	16.10	Cs	4.21	2.47	1.61
$\text{TFe}_2\text{O}_3$	1.83	1.66	2.51	Ba	2164	944	1856
MnO	0.03	0.02	0.05	La	11.9	39.2	54.0
MgO	0.40	0.37	0.53	Ce	18.3	57.9	93.3
CaO	1.30	0.44	0.51	Pr	1.92	6.37	10.7
$\text{Na}_2\text{O}$	2.23	3.12	4.27	Nd	6.95	21.4	39.5
$\text{K}_2\text{O}$	5.31	5.48	5.56	Sm	1.13	3.18	6.49
$\text{P}_2\text{O}_5$	0.08	0.07	0.10	Eu	0.48	0.77	1.62
LOI	1.98	0.99	1.30	Gd	1.29	3.23	5.67
Be	2.12	1.74	2.58	Tb	0.14	0.38	0.78
V	18.3	17.1	20.8	Dy	0.79	1.99	4.03
Cr	3.11	6.96	1.15	Ho	0.15	0.42	0.82
Co	1.69	1.89	0.90	Er	0.54	1.23	2.34
Ni	1.66	5.31	1.29	Tm	0.089	0.20	0.36
Cu	4.68	4.27	5.35	Yb	0.56	1.21	2.23
Zn	29.8	24.6	42.8	Lu	0.086	0.21	0.34
Ga	11.2	11.9	15.9	Hf	5.82	3.51	8.14
Rb	88.2	125	102	Ta	0.92	1.34	1.54
Sr	53.1	202	84.9	Pb	18.9	18.4	17.2
Y	4.83	11.8	19.7	Th	1.98	11.5	8.71
				U	0.78	1.32	1.64

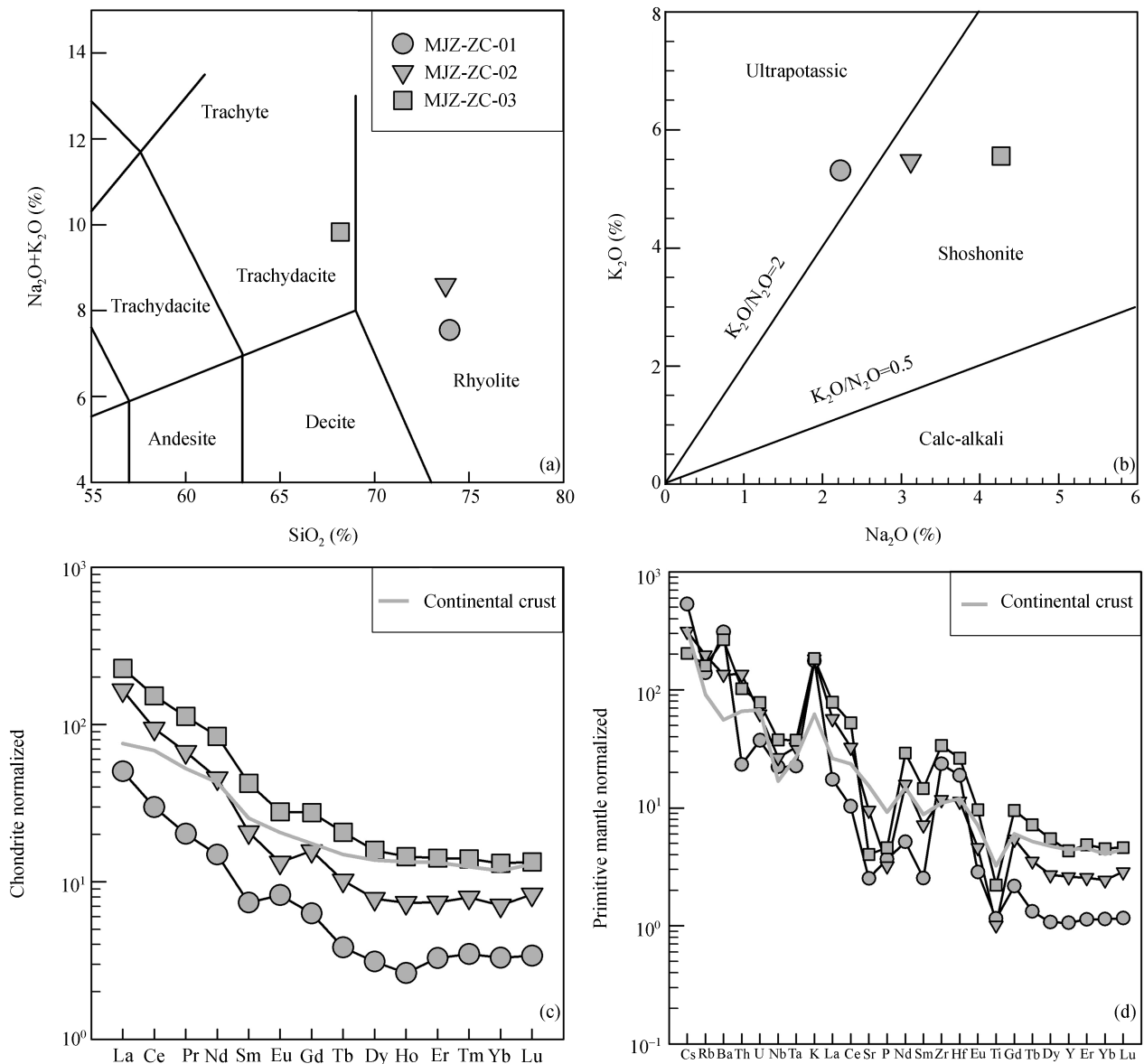


**Figure 4** Diagrams of total alkali to silica (a), Na<sub>2</sub>O vs. K<sub>2</sub>O (b), REE normalization (c) and elemental primitive mantle normalization (d) for zir-con-hosted Qingshan volcanic rocks from the Jiaozhou basin.

respectively, have been documented by previous works. The Mengyin potassic rocks were dated at  $124.3 \pm 0.6$ – $114.8 \pm 0.6$  Ma<sup>[25]</sup> and  $119.6 \pm 3.7$  Ma<sup>[26]</sup> using methods of <sup>39</sup>Ar-<sup>40</sup>Ar and Rb-Sr, respectively, while those in the Wulian area were given an age range of  $109.9 \pm 0.6$ – $108.2 \pm 0.6$  Ma using <sup>39</sup>Ar-<sup>40</sup>Ar method<sup>[27]</sup>. Coupled with the data by this study, it reveals a decreasing trend in age for the Qingshan potassic rocks from the western subregion eastward within Shandong Province, which approves what was proposed by previous workers<sup>[27]</sup>. However, high precision U-Pb dating using *in situ* zircon analysis for the Qingshan volcanic rocks and the

Mesozoic high-K magmatism, later than 100 Ma in East China, is first applied and reported by this study.

The Qingshan volcanic rocks compose the Mesozoic ‘Shoshonite Province’ in East China<sup>[28]</sup>. The shoshonitic suites are characterized by mugearite, latite, trachyte, trachyandesite and high-K rhyolite in lithology, enriched in potassic as well as other LILEs and depleted in HFSEs of Nb, Ta, Ti and P in geochemistry, along with high <sup>87</sup>Sr/<sup>86</sup>Sr and low <sup>143</sup>Nd/<sup>144</sup>Nd ratios. These features are interpreted as resulting from source rocks suffering the intensive metasomatism of liquid or/and melt fluids prior to their partial melting<sup>[28–30]</sup>. Distributions of the

Mesozoic volcanic suites within the 'Shoshonite Province' are controlled along regional fracture belts in East China, i.e. the Tan-Lu and Yangtze fault zones. In addition to Shandong Province, the other major occurrences of the Mesozoic high-K suites are concentrated at the northern Huaiyang basin adjacent to the Tan-Lu zone and Ningwu, Lishui and Lucong basins along the Yangtze fault zone. Variable degrees of radiometric dating have been documented for these suites. Yang et al.<sup>[31]</sup> reported a U-Pb age of  $131 \pm 5$  Ma and a Rb-Sr age of  $128 \pm 1$  Ma for the potassic volcanics from the Maotanchen Fm. in the northern Huaiyang basin. Later on the same suite was dated at  $127.1 \pm 3.6$  Ma ( $^{39}\text{Ar}$ - $^{40}\text{Ar}$ )<sup>[32]</sup> and  $148.8 \pm 2.5$  and  $138.3 \pm 2.2$  Ma (K-Ar) for the lower and upper parts of the stratum, respectively<sup>[33]</sup>. Qiu et al.<sup>[32]</sup> also reported an age range of  $103.7 \pm 2.8$  to  $94.0 \pm 2.6$  Ma for high-K lavas from the Xianghongdian Fm. (also called Xiaotian Fm.) in the northern Huaiyang basin, but the same suite was dated at  $132.2 \pm 2.1$  to  $116.2 \pm 1.8$  Ma by Wang et al.<sup>[33]</sup>. Although the 30–10 Ma difference between the data by these two works is obviously out of the analytical error limit, it is still evidently indicated that the timing of the potassic volcanic rocks in the Dabie Orogen and northern Huaiyang basin is older than those of the Qingshan Group in Shandong Province, backed by a zircon U-Pb age of  $129.2 \pm 2.6$  Ma for the Mesozoic trachyandesite in the North Dabie belt<sup>[34]</sup>. In addition, ages of  $140.1 \pm 0.8$  to  $126 \pm 3.4$  Ma ( $^{39}\text{Ar}$ - $^{40}\text{Ar}$ ) for a high-K suite from the Luzong basin were reported<sup>[35]</sup>, whereas those from the Ningwu basin were dated at  $131 \pm 4$  to  $127 \pm 3$  Ma using SHRIMP zircon U-Pb<sup>[36]</sup>, which also indicates that the potassic volcanic rocks exposed along the Yangtze fault zone are older than those of the Qingshan suite in eastern Shandong.

The Mesozoic-Cenozoic subcontinental lithospheric thinning and regional tectonic transform in East China were coupled with regional magmatism. The magmatic activities were featured by an abrupt change in source rocks parental to basaltic lavas from SCLM to asthenospheric mantle, and the reason for such a change has been interpreted as subcontinental lithospheric delamination followed by ascending erosion of asthenospheric flux. Yan et al.<sup>[37]</sup> dated the Daxizhuang alkaline basalt within the Jiaolai basin of eastern Shandong at  $73.5 \pm 0.3$  Ma using  $^{39}\text{Ar}$ - $^{40}\text{Ar}$  method. Coupled the  $\varepsilon_{\text{Nd}}(t)$  values of +7.5 to +7.6, a period of 120–73 Ma was suggested to represent the lithospheric thinning time in

East China. In fact, the asynchrony among the potassic volcanic rocks in East China is also recognized for the alkaline (with minor tholeiitic) basalts originated from the asthenospheric mantle, i.e. the timing for the alkaline basalts occurring at the northern Huaiyang basin and along the Yangtze fault zone is Cenozoic dominantly, with a maximum age of  $\sim 65$  Ma<sup>[13]</sup>, which is distinctly later than those exposed at eastern Shandong.

The continental dynamic significance embodied in the Mesozoic-Cenozoic tectono-magmatic events in East China interests the global geologists, however, our understandings on the mechanism and detailed processes of subcontinental lithospheric thinning, are still insufficient. For instance, though diverse petrogeneses have been argued for the potassic rocks (e.g. [29, 30] and references therein), and regional variation trend in compositions of source rocks parental to the Cenozoic alkaline basalts (e.g. melt mixtures of asthenospheric mantle with SCLM character of EM I and EM II, respectively, have been recognized for alkalic basalts located at the North China craton and the South China block<sup>[8,13–15,38]</sup>) have been documented, these findings and proposed models are still unsatisfactory to coincide with the present constraints mentioned above from radiometric geochronology and geochemistry of the Mesozoic-Cenozoic volcanic suites in East China. For a geodynamic view, to learn the reason and mechanism of the Mesozoic-Cenozoic tectonic transformation in East China, detailed investigations on timing, spatial distribution and chemical variation of diverse magmatic suites are especially essential. The Mesozoic high-Mg andesite and dacite are exposed along the northern margin of the North China craton in western Liaoning Province ( $159 \pm 3$  Ma for Xinglongou Fm.<sup>[12]</sup>;  $134.6 \pm 2.0$  Ma for Yixian Fm.<sup>[15]</sup>). Studying these volcanic suites, Gao et al.<sup>[12]</sup> recently revealed geochemical evidence for a petrogenesis by re-melting of eclogitic rocks foundered into upper mantle followed by their delamination from lower crust, which provided substantial message and research clue to understanding the dynamic processes of Mesozoic to Cenozoic subcontinental lithospheric evolution in northern North China as well as the whole North China craton. It is worth noticing that alkaline basalt sourced from asthenospheric mantle exposed at the northern North China craton was dated at  $100.4 \pm 1.6$  Ma<sup>[15]</sup>, which is distinctively older than those in Shandong Province. Mesozoic high-Mg andesitic suites were also recognized

recently by the present authors (in preparation), which is expected to provide messages on the genesis of the volcanic lavas and additional geochemical constraint on the evolution mechanism of the lower lithosphere beneath central East China.

*The authors are grateful to Liu Mingwei with the No.4 Institute of Geological and Mineral Resource Survey of Shandong Province for his assistance in the field trip. Dr. Hu Zhaochu with the Geological Department, Northwest University is thanked for his zircon U-Pb analysis. Comments of two anonymous referees significantly improved the manuscript.*

- 1 Gao S, Jin Z M. Delamination and its geodynamical significance for the crust-mantle evolution. *Geol Sci Tech Inform* (in Chinese with English abstract), 1997, 16: 1–9
- 2 Kay R W, Kay S M. Delamination and delamination magmatism. *Tectonophysics*, 1993, 219: 177–189
- 3 Rudnick R L. Making continental crust. *Nature*, 1995, 378: 571–578
- 4 Houseman G. From mountains to basin. *Nature*, 1996, 379: 771–772
- 5 Gao S, Zhang B R, Jin Z M, et al. How mafic is the lower continental crust? *Earth Planet Sci Lett*, 1998, 106: 101–117
- 6 Gao S, Kern H, Jin Z M, et al. Poisson's ratio of eclogite: Implications for lower crustal delamination of orogens. *Sci China Ser D-Earth Sci*, 2003, 46(9): 909–918
- 7 Furman T, Graham D. Erosion of lithospheric mantle beneath the East African Rift system: geochemical evidence from the Kivu volcanic province. *Lithos*, 1999, 48: 237–262
- 8 Fan Q C, Hooper P R. The Cenozoic basaltic rocks of Eastern China: Petrology and chemical composition. *J Petrology*, 1991, 32: 765–810
- 9 Fan W M, Menzies M A. Destruction of aged lower lithosphere and asthenosphere mantle beneath eastern China. *Geotectonica et Metallogenia*, 1992, 16: 171–179
- 10 Menzies M A, Fan W M, Zhang M. Palaeozoic and Cenozoic lithoprobes and the loss of >120 km Archean lithosphere, Sino-Korean craton, China. *Geological Society of London, Special Publication*, 1993, 76: 71–814
- 11 Zhai M G, Meng Q R, Liu J M, et al. Critical period of transforming of the Mesozoic tectonic system in eastern North China. *Sci China Ser D-Earth Sci* (in Chinese), 2003, 33(10): 913–920
- 12 Gao S, Rudnick R, Yuan H L, et al. Recycling lower continental crust in the North China craton. *Nature*, 2004, 432: 892–897
- 13 Chung S L. Trace element and isotope characteristics of Cenozoic basalts around the Tan-Lu Fault with implication for the eastern plate boundary between north and south China. *J Geol*, 1999, 107: 301–312
- 14 Zou H B, Zindler A, Xu X S, et al. Major, trace element, and Nd, Sr and Pb isotope studies of Cenozoic basalts in SE China: Mantle sources, regional variations and tectonic significance. *Chem Geol*, 2000, 171: 33–47
- 15 Zhang H F, Sun M, Zhou X H, et al. Secular evolution of the lithosphere beneath the eastern North China Craton: Evidence from Mesozoic basalts and high-Mg andesites. *Geochim Cosmochim Acta*, 2003, 67: 4373–4387
- 16 Bureau of Geology and Mineral Resources of Shandong Province. *Region Geology of Shandong Province* (in Chinese with English abstract). Beijing: Geological Publishing House, 1991. 597
- 17 Menzies M A, Xu Y G. Geodynamics of the north China Craton. In: Flower M, Chung S L, Lo C H, eds. *Mantle Dynamics and Plate Interactions in East Asia*, American Geophysical Union, Washington, DC, 1998. 155–165.
- 18 Chen Y X, Chen W J, Zhou X H, et al. Geochronology, Geochemistry and Tectonic Setting of the Mesozoic Volcanic Rocks in Northern Liaoning Province and Its Adjacent Areas (in Chinese). Beijing: Seismological Press, 1997. 1–279
- 19 Ren J Y, Tamaki K, Li S T, et al. Late Mesozoic and Cenozoic rifting and its dynamics setting in eastern China and adjacent areas. *Tectonophysics*, 2002, 344: 175–205
- 20 Zhang Z Q, Liu W M. *Lithostratigraphy of Shandong Province* (in Chinese). Wuhan: China Univ Geosci Press, 1996, 207–254
- 21 Liu M W, Zhang Q Y, Song W Q. Division of the Cretaceous lithostratigraphy and volcanic sequences of Shandong. *J Stratigraphy* (in Chinese with English abstract), 2003, 27(3): 247–253
- 22 Andersen T. Correction of common lead in U-Pb analyses that do not report <sup>204</sup>Pb. *Chem Geol*, 2002, 192: 59–79
- 23 Ludwig K R. *Isoplot/Ex, rev. 2.49. A geochronological toolkit for Microsoft Excel*. Berkeley Geochronology Center, Special Publication No. 1a, 2001, 1–56
- 24 Sun S S, McDonough W F. Chemical and isotopic systematics of oceanic basalts: implications for mantle composition and processes. In: Saunders A D, Norry M J, eds. *Magmatism in the Ocean Basins*. *Geol Soc Special Pub*, 1989. 313–345
- 25 Qiu J S, Xiu X S, Luo C H. Potash-rich volcanic rocks and lamprophyres in western Shandong Province: <sup>40</sup>Ar-<sup>39</sup>Ar dating and source tracing. *Chin Sci Bull*, 2002, 47(2): 91–99
- 26 Qiu J S, Wang D Z, Zhou J C, et al. Geology, geochemistry and genesis of the Mesozoic shoshonitic volcanic rocks in Shandong Province. *Earth Sci — J China Univ Geosci* (in Chinese with English abstract), 1996, 21(5): 546–552
- 27 Qiu J S, Wang D Z, Luo Q H, et al. <sup>40</sup>Ar-<sup>39</sup>Ar dating for volcanic rocks of Qingshan Formation in Jiaolai basin, eastern Shandong Province: a case study of the Fenlingshan volcanic apparatus in Wulian County. *J China Univ* (in Chinese with English abstract), 2001, 7(30): 351–355
- 28 Wang D Z, Ren Q J, Qiu J S, et al. Characteristics of volcanic rocks in the Shoshonite Province, eastern China, and their metallogenesis. *Acta Geol Sin* (in Chinese with English abstract), 1996, 70(1): 23–34

- 29 Fan W M, Guo F, Wang Y J, et al. Late Mesozoic volcanism in the northern Huaiyang tectono-magmatic belt, central China: partial melts from a lithospheric mantle with subducted continental crust relicts beneath the Dabie orogen? *Chem Geol*, 2004, 209: 27–48
- 30 Qiu J S, Jiang S Y, Zhang X L, et al. Petrogenesis of K-enriched volcanic rocks on the northern and southern sides of the Dabie-Sulu Orogenic belt, East China: constraints from trace elements and Sr-Nd-Pb isotopes. *Acta Geosci Sin* (in Chinese with English abstract), 2004, 25(2): 255–262
- 31 Yang Z L, Shen J L, Shen W Z, et al. Isotopic geochronological study on timing of the Mesozoic volcanic-intrusive rocks in northern Huaiyang. *Geol Review* (in Chinese with English abstract), 1999, (suppl): 674–680
- 32 Qiu J S, Luo Q H, McInnes B. Later Mesozoic high-K magmatism in central southern section of the Tan-Lu Fault and its controls on the golden (-copper) mineralization. *Mineral Geol* (in Chinese with English abstract), 2002, 21(Supp.): 211–214
- 33 Wang Y J, Fan W M, Guo F. K-Ar dating of late Mesozoic volcanism and geochemistry of volcanic gravels in the North Huaiyang Belt, Dabie orogen: Constraints on the stratigraphic framework and exhumation of the Morthem Dabie orthogneiss complex. *Chin Sci Bull*, 2002, 47(20): 1688–1695
- 34 Xue H M, Dong S W, Liu X C. U-Pb zircon dating for Cretaceous adakitic volcanic rocks in eastern part of the North Dabie Mountains. *Geochimica* (in Chinese with English abstract), 2002, 31(5): 455–463
- 35 Liu H, Qiu J S, Lo C H, et al. Petrogenesis of the Mesozoic potash-rich volcanic rocks in the Luzong basin, Anhui Province: geochemical constraints. *Geochimica* (in Chinese with English abstract), 2002, 31(2): 129–140
- 36 Zhang Q, Jian P, Liu D Y, et al. SHRIMP zircon dating on the Ningwu volcanic suite and its significance. *Sci China Ser D-Earth Sci* (in Chinese), 2003, 33(4): 309–314
- 37 Yan J, Chen J F, Xie Z, et al. Mantle xenoliths from late Cretaceous basalt in eastern Shandong Province: New constraint on the timing of lithospheric thinning in eastern China. *Chin Sci Bull*, 2003, 48(19): 2139–2144
- 38 Xu Y G, Menzies M A, Matthey D P, et al. The nature of the lithospheric mantle near the Tancheng-Lujiang fault, China: An integration of texture, chemistry and isotopes. *Chem Geol*, 1996, 134: 67–81